DIFFRACTION BREAK-UP OF DEUTERONS

Translated and reprinted from Coll. sci. works "Diffraction Interaction of Hadrons with Nuclei" (Naukova dumka, Kiev, 1987), pp. 442–237

O.F. NEMETS

Institute for Nuclear Research, National Academy of Sciences of the Ukrainian SSR
(Kyiv, Ukraine)

The results of studies of the break-up of deuterons in the field of nuclei with different masses are reviewed. The data obtained in kinematically complete experiments are analyzed within the diffraction model. It is ascertained that the differential cross-section of the deuteron break-up non-monotonously varies with the change of the mass number of nuclei, which can be explained by the difference of their surface diffuseness. The relation of isotope-isotone effects to the diffuseness of a nucleus surface revealed while studying the dependence of the total cross-sections of reactions on the neutron excess is analyzed as well.

On the interaction with nuclei, a deuteron has high probability of the break-up into a proton and a neutron already at comparatively low energies. The high probability of such a process is caused by the low binding energy of a deuteron (2.23 MeV), large size ("looseness"), and noncoincidence of the charge and gravity centers. For the first time, the process of deuteron break-up in the electric field of a nucleus was theoretically studied in 1935 by Oppenheimer [1]. Then the process has been studied by many authors [2–7]. In 1955, Akhiezer and Sitenko [8], Feinberg [9], and Glauber [10] have independently suggested the diffraction mechanism of deuteron break-up. For the diffraction break-up to occur, the needed energy and momentum must be transferred to the deuteron in the process of interaction with a nucleus. This can be achieved if the energy of an incident deuteron meets the following condition: $E_d \gg 0.2A^{2/3}$ MeV. For nuclei with medium atomic weights ($A \approx 60$), the value $0.2A^{2/3}$ is approximately equal to three. Therefore, at deuteron energies exceeding 10 MeV, the condition $E_d \gg 0.2A^{2/3}$ MeV starts to be fulfilled.

The break-up of a deuteron can both be the process of direct break-up and the process of stripping with the capture of one of the nucleons into an unbound state of the nucleus and its subsequent emission.

Despite the fact that the process of deuteron break-up was predicted in 1935, it has not been observed in kinematically complete experiments till the early 1960s, though indirect indications of its existence were obtained somewhat earlier. The first experimental indications of the noticeable probability of such a process were obtained during the research of the elastic scattering of deuterons by heavy nuclei [11–15]. Under conditions of validity of the quasiclassical approximation (the Sommerfeld parameter $n = \frac{Ze^2}{\hbar v} \gg 1$), the fast reduction of the elastic scattering cross-section in comparison with the Rutherford scattering one was observed starting from angles $\theta_{\rm cr}$ which correspond to the radius of interaction $R_{\rm int}$ significantly exceeding the sum of the nucleus and deuteron radii,

$$\sin(\theta_{\rm cr}/2) = Ze^2/(mv^2 R_{\rm int} - Ze^2). \tag{1}$$

This phenomenon can be explained only by the deuteron break-up.

In work [13], the break-up cross-section was estimated, and it gave the differential cross-section amounting to several hundreds of mb/sr. A detailed study of the break-up process requires kinematically complete experiments. As is generally known, the complete kinematics in reactions with three particles in the exit channel is determined by three projections of the momentum for each of three particles, i.e. by nine kinematic quantities. The law of conservation of the energy-momentum reduces the number of the kinematic quantities that must be determined in experiments to five. These requirements can be met by the simultaneous registration of a neutron and a proton at fixed angles θ_n and θ_p with the measurement of their energies. It should be noted that, in order to obtain reliable data, the registration devices must satisfy strict requirements: a time resolution of $(1 \div 2) \times 10^{-9}$ s, a fine resolution in energy, including that for registered neutrons, etc.

The equipment satisfying these requirements was designed in the departments of nuclear electronics and nuclear reactions of the Institute of Physics, Academy of Sciences [16, 17] of Ukrainian SSR, in the early 1960s. In 1962, the first kinematically complete experiments were performed. The neutron energy was measured by the time-of-flight method.

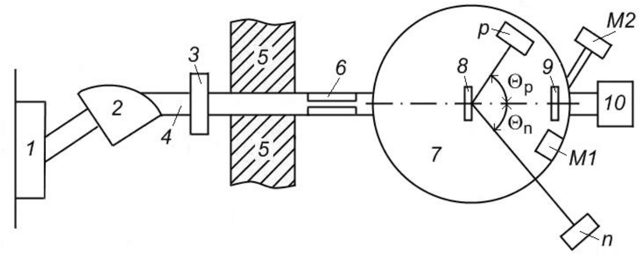

Fig. 1. Experimental set-up

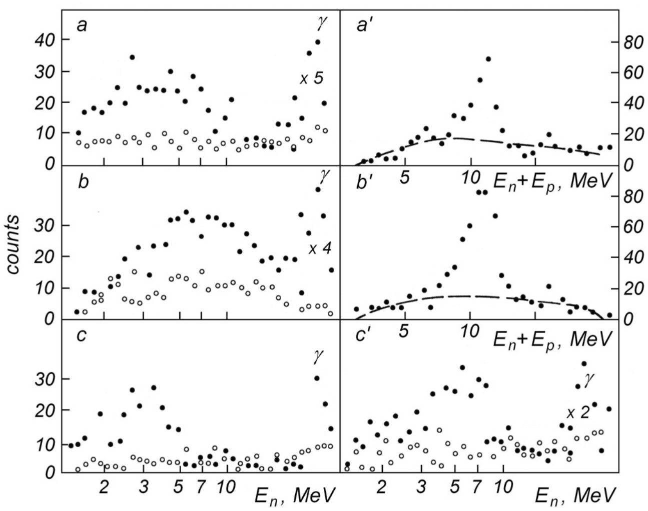

Fig. 2. Spectra of neutrons (a, b, c, c') and the total energy of a neutron and a proton registered in coincidence (a', b'). White circles and dashed lines mark the background of accidental coincidences. The gamma-peak is marked by γ

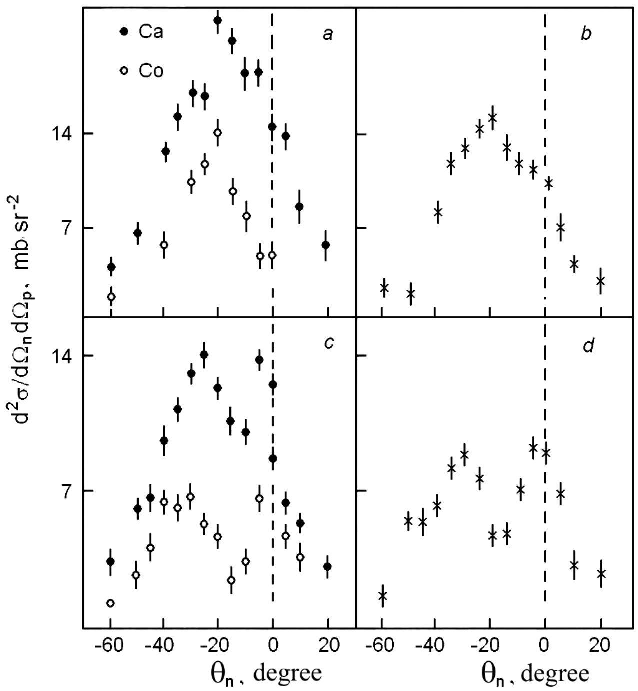

Fig. 3. Angular $n-p$-correlations on the break-up of deuterons with an energy of 13.6 MeV on the interaction with nuclei of calcium (black dots), cobalt (white dots) and titanium (crosses) for different adjustment angles of a spectrometer of protons (a, c – $\theta_p = 30°$; b, d – $\theta_p = 40°$)

In experiments, a spectrometer of protons was set under a fixed angle, while the adjustment angle of a neutron spectrometer was changed. The spectra of neutrons and protons were measured in coincidences as functions of the angle between the emission directions of a neutron and a proton.

Figure 1 shows the experiment geometry. Here, *1* – cyclotron; *2* – magnet that deflects the deuteron beam; *3*, *6* – collimators; *4* – ion guide; *5* – shielding wall; *7* – measuring chamber; *8* – work target; *9* – golden target for monitoring; *10* – Faraday cup; *M1* – monitor that registers deuterons elastically scattered by the work target; *M2* – monitor that registers deuterons elastically scattered by the golden target; *P* – semiconductor spectrometer; *n* – toluylene neutron detector located by 71 cm away from a target to measure the neutron energy by the time-of-flight method.

Figure 2 presents the spectra of neutrons registered [16, 18] in coincidences with protons (a, b, c, c', and the spectra of the total energy of the coinciding neutron and proton (a', b'). The spectra correspond to different detection angles of neutrons and protons, as well as to different energy intervals of registered protons: a, a' – θ_p=40°, θ_n = –35°; b, b', c, c' – θ_p=30°, θ_n = –20°; a, b – 3 MeV $\leq E_p \leq$ 9 MeV; c – 6.7 MeV $< E_p <$ 8.4 MeV; c' – 5 MeV $< E_p <$ 6.7 MeV. In the total energy spectra of the coinciding neutron and proton, the peak that corresponds to the primary deuteron energy after the subtraction of its binding energy ($E_p + E_n = E_d - E_{bd}$ = 11.4 MeV) can be clearly seen.

The presence of the pronounced maximum in the total energy spectra indicates that, after the break-up reaction, the target nucleus remains in the ground state. For medium-weight nuclei, the spectra of neutrons and protons, as well as the angular correlations, turned out to be similar [16, 18–23]. Figure 3 demonstrates the angular $n-p$-correlations of the deuteron break-up on the interaction with nuclei of calcium, cobalt, and titanium. The angular correlation is characterized by two maxima, one of which is located at an angle close to zero, while the second – at the angle close to the adjustment angle of the proton spectrometer, but to the opposite side relative to the direction of the incident deuteron beam. That is, the position of the second maximum changes with the change of the adjustment angle of the proton spectrometer. In work [19], the zero-angle maximum on the deuteron break-up on a nickel target of the natural composition is satisfactorily described by the Butler stripping reaction theory [24] for the proton capture in unbound states of the nucleus at $l = 0$, 1, 2 with contributions of 1; 0.3; 0.1, respectively. As for the second maximum, it can be referred to the diffraction break-up mechanism despite the relatively low energy of deuterons.

By the time of the execution of experiments, the theory of diffraction break-up was developed by A.G. Sitenko and his apprentices [25–28] in detail, which made possible the comparison of theory and experiment.

The diffraction break-up cross-section has the form [28]

$$\frac{d^3\sigma}{d\Omega_n d\Omega_p dE_p} = \frac{\alpha^2 m k_p}{(2\pi)^3 \hbar^2 \varepsilon k^2} \times$$

$$\times \sqrt{2E_d(E_d - \varepsilon - E_p)}\, |f_d(\Delta, \mathbf{u}, \theta)|^2 \,, \quad (2)$$

where E_d, E_p, $\mathbf{k}$, $\mathbf{k}_p$ – kinetic energies and wave vectors of a deuteron and a proton, respectively; m – nucleon mass; $\alpha = \left(\frac{m\varepsilon}{\hbar^2}\right)^{1/2} = \frac{1}{2R_d}$; R_d – deuteron radius, ε – binding energy of a deuteron; and the diffraction break-up amplitude

$$f_d(\Delta, \mathbf{u}, \theta) = f_d(\mathbf{u}, \theta) \exp\left(-\frac{\Delta^2 x^2}{4R_0^2}\right), \quad (3)$$

$$f_d(\mathbf{u}, \theta) = ikR_0^2 \left(\frac{R_d}{R_0}\right)^2 \frac{8\sqrt{2\pi}}{3\alpha^{3/2}} \frac{1}{(1-u^2)^3} \times$$

$$\times \Big[\left(1 + \frac{u^2}{2} - \frac{3}{2}u_z^2 - iu\right) J_0(x) -$$

$$-\frac{3}{2}(u^2 - u_z^2) \cos 2\varphi J_2(x) \Big]. \quad (4)$$

Here, $\mathbf{u}$ – vector of the relative velocity between a neutron and a proton; u_z – projection of the vector $\mathbf{u}$ on the z axis (direction of the deuteron beam); φ – azimuth angle of the vector $\mathbf{u}$; and Δ – diffuseness parameter.

Figure 4 shows the measured angular $n-p$-correlations on the interaction of deuterons with an energy of 13.6 MeV with isotopes ^{60}Ni (*1*) and nuclei of Cu (*2*) of the natural composition, as well as the results of calculations by diffraction theory (solid curves) [28]. The theory does not provide the quantitative description of experimental cross-sections. Therefore, the theoretical curves were normalized to experimental data. Moreover, the theoretical curves were several degrees shifted in order to overlap the positions of the maxima. Taking a relatively low energy of deuterons into account (E_d exceeded the value of $0.2A^{2/3}$ only by four times), the agreement of theory with experiment can be deemed satisfactory. On this ground, the reaction cross-section corresponding to the second maximum can be attributed to the diffraction break-up mechanism. Thus, the basic mechanisms of break-up of deuterons with an energy of 13.6 MeV by medium-weight nuclei are diffraction break-up, stripping, and capture of one of the nucleons into an unbound state of the nucleus and Coulomb break-up.

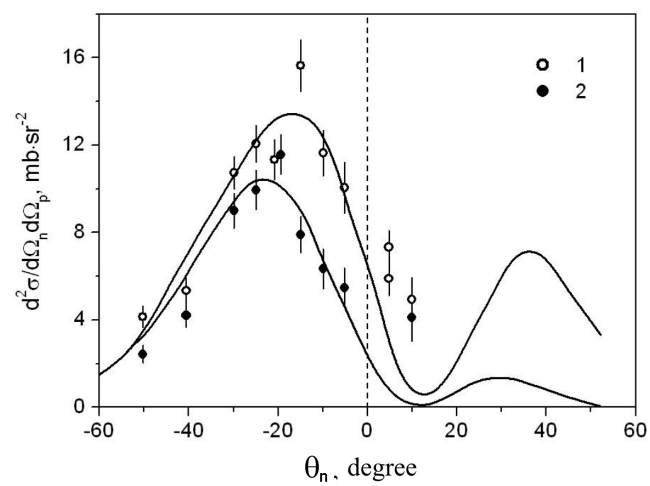

Fig. 4. Angular $n-p$-correlations at break-up of deuterons in the process of interaction with nuclei of ^{60}Ni (*1*) and $^{\rm nat}$Cu (*2*)

Figures 3 and 4 illustrate the significant difference of the cross-sections of break-up reactions on nuclei with similar values of Z and A. Such a difference can be explained by the assumption that nuclei, on the interaction with which the break-up was studied, had noticeably different diffusenesses of the surface layers. The influence of diffuseness upon the diffraction break-up process was prognosticated for the first time by A. Sitenko and V. Tartakovsky [26] who found that the diffraction break-up cross-section changes by one order of magnitude with increase in the diffuseness parameter Δ from 0 to $\Delta = R$. The influence of diffuseness was also taken into account in work [28]. Experiments on

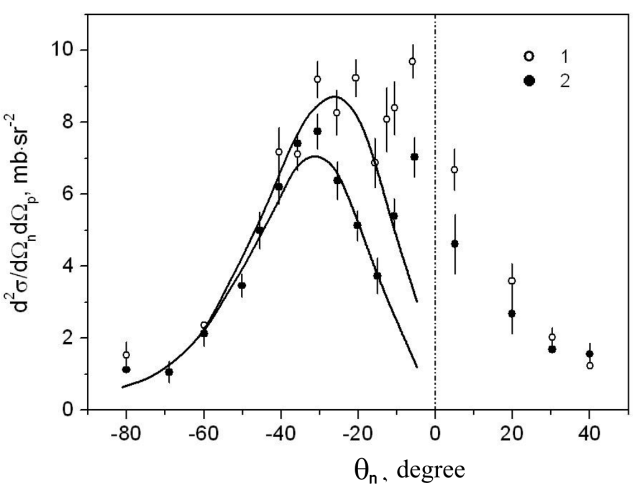

Fig. 5. Angular $n-p$-correlations on the deuteron break-up due to the interaction with nuclei ^{58}Ni (*1*) and ^{64}Ni (*2*). Solid curves mark the results of calculations by diffraction theory. The diffuseness parameters for ^{58}Ni and ^{64}Ni are equal, respectively, to 1 and 3 fm

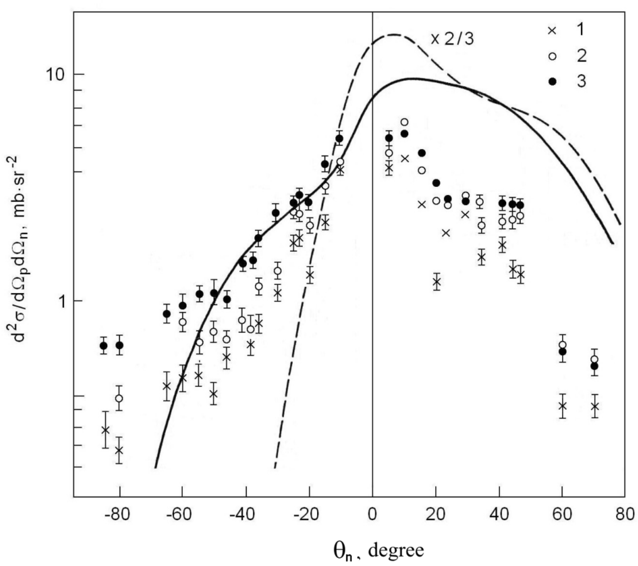

Fig. 6. Angular $n-p$-correlations on the break-up of deuterons with an energy of 13.6 MeV by nuclei ^{197}Au (*1*), ^{207}Pb (*2*), and ^{208}Pb (*3*). The adjustment angle of a spectrometer of protons is 70°. The dashed curve represents the results of calculations by the Landau–Lifshits theory without taking the interaction of a neutron and a nucleus into account; the solid curve shows the results of calculations by the Landau–Lifshits theory with consideration of the neutron-nucleus interaction

separated isotopes of nickel were carried out for both a further verification of the assumption about the influence of the diffuseness of a nucleus on the diffraction break-up cross section and the exclusion of a possible influence of the nucleus charge on this process. It was assumed that the diffuseness parameter can increase with moving away from the magic number 28, i.e. with increase in the excess of neutrons. As seen from Fig. 5, where the $n-p$-correlations on the break-up of deuterons by nuclei ^{58}Ni and ^{64}Ni are shown, the cross-section of this process is much less for nucleus ^{64}Ni than for nucleus ^{58}Ni. After publishing the above-presented results, the kinematically complete experiments were repeatedly performed in a number of foreign laboratories both on the above-stated and other nuclei and at other energies [29–32]. The energy spectra, absolute cross-sections, and angular correlations obtained in those works are in agreement with the Kyiv results.

In connection with the discovered noticeable difference between the deuteron break-up cross-sections by medium-weight nuclei, it was of interest to study whether similar effects take place for heavy nuclei, where the main contribution at an energy of 13.6 MeV must be given by the Coulomb break-up. With this purpose, the experimental studies of the spectra and angular correlations of products of the deuteron break-up by nuclei ^{197}Au, ^{207}Pb, ^{208}Pb, $^{\rm nat}$Pb, and Bi were performed [33–37].

Figure 6 shows the angular $n-p$-correlations on the deuteron break-up in the process of interaction with nuclei ^{197}Au, ^{207}Pb, and ^{208}Pb. The cross-section is maximum on the interaction with twice magical nuclei ^{208}Pb. However, the difference between the cross-sections is not so large as that for medium-weight nuclei.

The results of calculations by the Landau–Lifshits theory of Coulomb break-up, which are shown in Fig. 6 by the dotted curve, do not give a satisfactory description of experiments. In a number of works, it was noted that, on the Coulomb break-up at a deuteron energy close to the Coulomb barrier, the significant role must be played by the interaction of neutrons with nuclei [33, 34, 38]. The calculations by the Landau–Lifshits theory [3] were performed in work [35], where the potential elastic scattering of neutrons by a nucleus was taken into account, and the optical potential was taken from work [39]. In [35], the wave function of a neutron in the final state, in contrast to [3] where it was planar, was taken in the form suggested in [38, 40] as

$$\psi_n(\mathbf{r}_n) = \exp(i\mathbf{k}_n\mathbf{r}_n) + f(\widehat{\mathbf{k}_n\mathbf{r}_n})\frac{\exp(i\mathbf{k}_n\mathbf{r}_n)}{r_n}, \qquad (5)$$

where the amplitude of neutron elastic scattering on a nucleus

$$f(\widehat{\mathbf{k}_n\mathbf{r}_n}) = \frac{i}{2k_n}\sum_{i_n=0}^{\infty}(2l_n+1)(1-S_{\text{in}})P_{\text{in}}\cos(\widehat{\mathbf{k}_n\mathbf{r}_n}). \quad (6)$$

In this case, the differential cross-section of deuteron break-up in the approximation of zero-range nuclear forces acting between the nucleons in a deuteron has the following form:

$$\frac{d^3\sigma}{d\Omega_p d\Omega_n dE_p} = 2\alpha\frac{\hbar}{\pi}\sqrt{m\varepsilon}k_n k_p\times$$

$$\times\Big[\int \psi_d^{(+)}(\mathbf{r})\psi_p^{(-)}(\mathbf{r})\exp(-i\mathbf{k}_n\mathbf{r})d\mathbf{r}+$$

$$+\int\frac{f(\mathbf{k}_n\mathbf{r})}{r}\exp(i\mathbf{k}_n\mathbf{r})\psi_d^{(+)}(\mathbf{r})\psi_p^{(-)*}(\mathbf{r})d\mathbf{r}\Big]^2. \quad (7)$$

The wave functions of a deuteron $\psi_d^{(+)}(\mathbf{r})$ and a proton $\psi_p^{(-)*}(\mathbf{r})$ are taken from work [3]:

$$\psi_d^{(+)}(\mathbf{r}) = \frac{1}{\sqrt{v_d}}\exp\left(-\frac{\pi n_d}{2}\right)\Gamma(1+in_d)\exp(i\mathbf{k}_d\mathbf{r})\times$$

$$\times F\left[-in_d, 1, i(k_d r - \mathbf{k}_d\mathbf{r})\right]; \quad (8)$$

$$\psi_p^{(-)*}(\mathbf{r}) = \frac{1}{(2\pi\hbar)^{3/2}}\exp\left(-\frac{\pi n_p}{2}\right)\Gamma(1+in_p)\exp(i\mathbf{k}_p\mathbf{r})\times$$

$$\times F\left[-in_p, 1, i(k_p r + \mathbf{k}_p\mathbf{r})\right]. \quad (9)$$

Here, $\mathbf{k}_n$, $\mathbf{k}_p$, $\mathbf{k}_d$ are the wave vectors of the neutron, proton, and deuteron, respectively; n_p, n_d – Coulomb parameters of the proton and the deuteron; v_d – deuteron velocity; m – nucleon mass; and ε – binding energy of the deuteron.

The first right-hand term in expression (7) describes the purely Coulomb deuteron break-up, and the second term takes the interaction of the neutron and a nucleus into consideration. This term can be estimated in the approximation $n_d \gg 1$ or $n_p \gg 1$, by using the stationary phase method for rapidly oscillating functions [41] and taking the slowly varying amplitude $f(\widehat{\mathbf{k}_n\mathbf{r}_n})$ outside the integral symbol as a function of the angle $(\widehat{\mathbf{k}_n\mathbf{r}_n})$ at

$$\theta = \theta_0, \quad \varphi = \varphi_0$$

$$\left(\varphi_0 = \pi, \quad \theta_0 = \mathrm{arctg}\,\frac{\sin\theta_p}{2\rho - \cos\theta_p}, \quad \rho = \frac{n_p}{n_d}\right).$$

The remaining integral can be taken analytically, and we get the following result:

$$I(\widehat{\mathbf{k}_d\mathbf{r}_p}) = \frac{\exp\{i\left[\arg(\Gamma(1+in_d)+\arg\Gamma(1+in_p)\right]\}}{\sqrt{v_d}(2\pi\hbar)^{3/2}}\times$$

$$\times\frac{8\pi^2\sqrt{n_d n_p}\exp\left[-\pi(n_d+n_p)\right]}{\left[(\mathbf{k}_d-\mathbf{k}_p)^2-\mathbf{k}_n^2\right](1+\xi)}\left[\frac{\mathbf{k}_p^2-(\mathbf{k}_d+\mathbf{k}_n)^2}{(\mathbf{k}_d-\mathbf{k}_p)^2-\mathbf{k}_n^2}\right]^{in_d}\times$$

$$\times\left[\frac{\mathbf{k}_d^2-(\mathbf{k}_p+\mathbf{k}_n)^2}{(\mathbf{k}_d-\mathbf{k}_p)^2-\mathbf{k}_n^2}\right]^{in_p}F(-in_d,-in_p,1-\xi), \quad (10)$$

where

$$\xi = \frac{4k_d k_p}{(\mathbf{k}_d-\mathbf{k}_p)^2-\mathbf{k}_n^2}\sin^2\frac{1}{2}(\widehat{\mathbf{k}_d\mathbf{r}_p}).$$

The results of calculations which the interaction of a neutron and a nucleus take into account are shown in Fig. 6. The consideration of the neutron-neutron interaction noticeably improves the description of experimental data, particularly in the region of negative angles, where the isotopic dependence of break-up cross-sections appears most strongly. This leads to the conclusion that, for heavy nuclei, the difference in break-up cross-sections on different nuclei and isotopes is related to the difference in the interaction cross-sections of neutrons and nuclei.

Unfortunately, there are few data in the literature on the measured cross-sections of elastic scattering of neutrons by isotopes of lead in the energy interval (2÷8) MeV. Therefore, nothing can be said about a possible difference in the cross-sections of the scattering of neutrons by nuclei ^{207}Pb and ^{208}Pb.

The calculations, in which the contributions of both the potential neutron scattering and the scattering with the formation of a compound nucleus were taken into account, have been carried out on the basis of the assumption that the cross-sections of the potential neutron scattering by nuclei ^{207}Pb and ^{208}Pb are close by magnitude, and the main difference in the cross-sections of the scattering on them is caused by different contributions of the formation of a compound nucleus [36, 37].

The potential scattering, as in [35], was described, by using the optical model, while the scattering with the formation of a compound nucleus was analyzed within the Hauser–Feshbach theory [42]. The theory supposes that the differential scattering cross-section for neutrons,

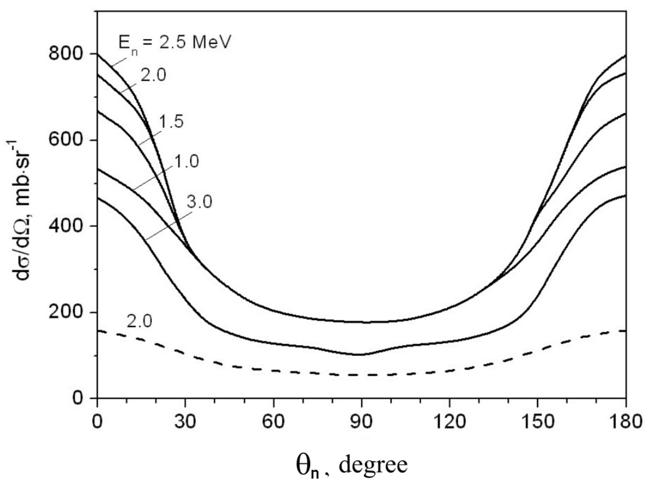

Fig. 7. Results of calculations of the differential cross-sections of elastic scattering with the formation of a compound nucleus by the Hauser–Feshbach theory. Solid curves – for nucleus ^{208}Pb (neutron energies are shown on the right-hand side of curves), dashed curves – for nucleus ^{207}Pb

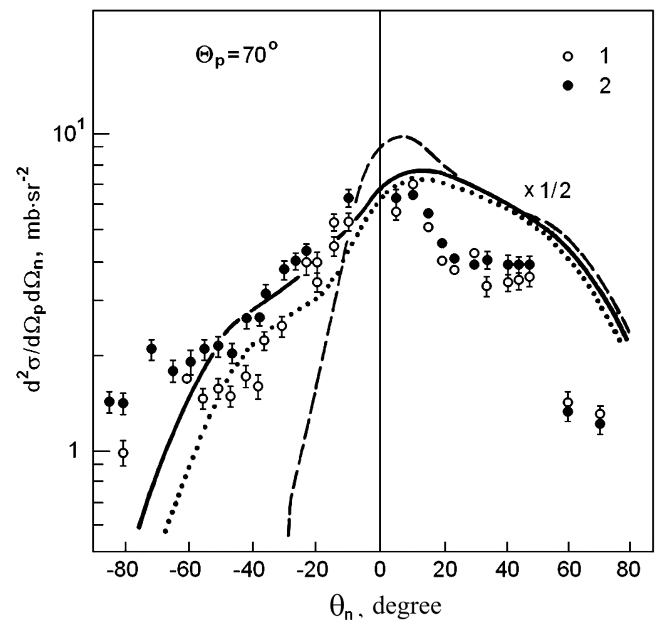

Fig. 8. Angular $n-p$-correlations on the break-up of deuterons with an energy of 13.6 MeV by isotopes of ^{207}Pb (*1*) and ^{208}Pb (*2*). The adjustment angle of a spectrometer of protons is 70°. Dashed curve – the result of calculations by the Landau–Lifshits theory; solid curve – results of calculations with regard for the elastic scattering (the potential one and that with the formation of a compound nucleus) of neutrons by nuclei ^{208}Pb; dotted curve – the same for ^{207}Pb

where the transition of the target nuclei from a state with spin J to a state with spin J' occurs, has the form

$$\sigma(J,J',\theta)=\frac{\lambda\!\!\!^{-2}}{8(2J+1)}\sum_l T_l(E)\sum_I\Big\{\sum_{J,l',l''}T_{l'}(E')\times$$

$$\times\Big|\sum_L Z(lIlI,iL)Z(l'Il'I,i'L)P_L(\cos\theta)\Big|/$$

$$/\sum_{l''E''}T_{l''}(E'')\Big\}. \tag{11}$$

Here, i is the channel spin for an incident neutron with energy E and orbital moment l; i',E', and l' – the same for the neutron in the final state; i'',E'',l'' – correspond to any neutron which can be emitted; $T_l(E)=1-|S_l|^2$ – the penetrability coefficient; and Z – Racah coefficients. The calculated differential cross-sections of elastic scattering with the formation of a compound nucleus are shown in Fig. 7.

The cross-section of elastic scattering with the formation of a compound nucleus is much larger for nucleus ^{208}Pb than that for nucleus ^{207}Pb. This indicates that the contribution of the process of neutron capture by a nucleus and its further emission into the elastic channel (registered as the deuteron break-up) will be higher for nucleus ^{208}Pb than that for ^{207}Pb. This leads to an increase of the break-up cross-section at near-threshold energies, which agrees with the experiment, as seen in Fig. 8.

In addition to the explanation of the change of the cross-sections of diffraction break-up of deuterons by medium-weight nuclei, the assumption about an increase of the diffuseness of nuclei when the numbers of neutrons and protons move away from magic numbers can also be applied to the explanation of other phenomena.

Such an attempt was made to explain the isotope-isotone effects in the total cross-sections of reactions [43, 44]. The isotope-effects consist in a disproportionate change of the total cross-sections of reactions with a change of the nucleus size and the Coulomb barrier penetrability, as it should be in the quasiclassical approximation, where

$$\sigma_R=\pi R^2\left(1-\frac{E_b}{E}\right)=$$

$$=\pi r_0^2\left(A_1^{1/3}+A_2^{1/3}\right)^2\left(1-\frac{E_b}{E}\right). \tag{12}$$

Here, E_b – the height of the Coulomb barrier; E – the energy of a projectile; r_0 – the radius parameter; A_1 –

the atomic weight of a target nucleus; A_2 – the atomic weight of the particle.

As seen from Fig. 9, the isotope-isotone effects in the total cross-sections of reactions appear for different projectiles and at different energies. For isotopes ^{48}Ti – ^{50}Ti, ^{54}Fe – ^{56}Fe, ^{58}Ni – ^{60}Ni – ^{62}Ni – ^{64}Ni, the cross-sections increase much faster than the radius of a target-nucleus, while, for isotones ^{50}Ti – ^{51}V – ^{52}Cr, the inverse picture is observed – the cross-sections decrease faster than the size of a target-nucleus.

These effects cannot be explained by a change of the Coulomb barrier penetrability or by a difference in the thresholds of reactions. For example, a change of the barrier penetrability at the fixed 12.6-MeV energy of deuterons (Fig. 9, dotted curve) correctly predicts the whole trend in the change of cross-sections, but does not influence the trend of the cross-sections for isotopes. As for the influence of reaction thresholds, they could have played their role in a change of the cross sections for alpha-particles, where all reactions have negative Q, and the reaction threshold (α, 2n) on ^{58}Ni is extremely high ($Q = -19.8$ MeV). However, as can be seen from Fig. 9, the isotope-isotone effects are preserved for all types of particles, including protons with an energy of 99 MeV.

The isotope-isotone effects can be seen against the background of the average dependence of reaction cross-sections on A in the form $\sigma_R = \pi r_0^2 A^{2/3}$ (Fig. 9, solid line), which allows one to attribute them to the influence of geometric factors. It should be noted that a change of the geometric parameters of nuclei (size, diffuseness magnitude, and deformation) cannot be linked only with the filling of shells; such a conclusion can be made from the fact that the total cross-sections for nuclei with the filled shell $N = 28$ significantly differ (^{50}Ti, ^{51}V, ^{52}Cr, ^{54}Fe).

The trends of the total reaction cross-sections for isotopes and isotones are defined in a great extent by the ratio of the numbers of neutrons and protons in nuclei; more specifically, by a magnitude of relative neutron excess.

Taking the relative neutron excess as a parameter, we will describe both the isotope and isotone effects. Figure 10 shows the experimental values of total cross-sections normalized to $A^{2/3}$ for different nuclei versus the relative neutron excess. The lines show the limits of the "error corridor" for isotopes of nickel.

As can be seen from Fig. 10, the values of total cross-sections in the range of experimental errors are within these "corridors" for all particles, for which both the isotope and isotone effects take place. The values of cross-sections can be described by the following empiric formula which takes the role of the relative neutron excess into account:

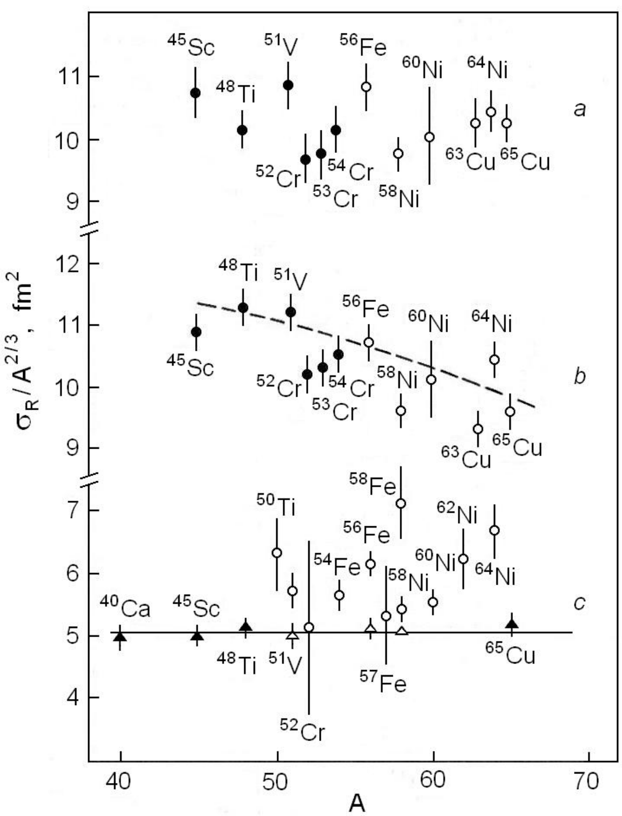

Fig. 9. Experimental values of reaction total cross-sections for deuterons with an energy of 13.6 MeV (a); alpha-particles with an energy of 27.2 MeV (b) and protons with energies of 60.8 and 99 MeV (c). Dashed curve reproduces the trend of the absorption cross-section in the quasiclassical approximation; solid line – the trend of the absorption cross-section for an absolutely black nucleus

$$\sigma_R = \left[\pi r_0^2 + \beta(N-Z)/A\right] A^{2/3}. \tag{13}$$

The parameter r_0 for deuterons with an energy of 13.6 MeV, alpha-particles with an energy of 27.2 MeV, and protons with an energy of 60.8 MeV has the following values: 1.76; 1.70, and 1.31 fm. The parameter β within the limits of errors does not depend upon the type of particles and their energy, and therefore it can be associated with fundamental properties of nuclei. By suggesting that the relative neutron excess influences the surface layer diffuseness, the total cross-sections of reactions for isotopes of nickel within the optical model of nuclei with parameters, which describe well the elastic

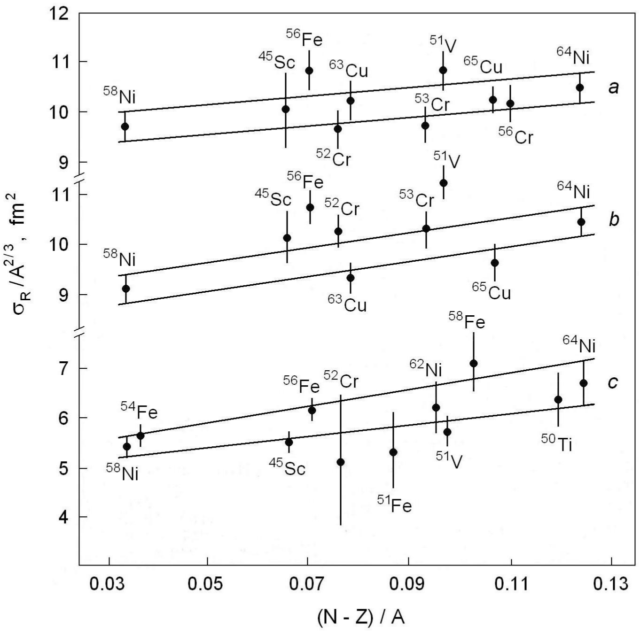

Fig. 10. Experimental total cross sections of reactions for deuterons with an energy of 13.6 MeV (a); alpha-particles with an energy of 27.2 MeV (b) and protons with an energy of 60.8 MeV (c) versus the neutron excess $(N-Z)/A$. Solid curves mark the "corridors of errors"

scattering of deuterons with an energy of 13.6 MeV on isotopes of nickel, were calculated in [45].

The optical potential has the form

$$V = -V_0 \left[1 + \exp\left(\frac{r - r_v A^{1/3}}{a_v} \right) \right] +$$

$$+ iW_0 \exp\left[- \left(\frac{r - r_w A^{1/3}}{a_w} \right) \right] \tag{14}$$

with the parameters $V_0 = 72$ MeV, $W_0 = 17$ MeV, $r_v = 1.35$ fm, $r_w = 1.27$ fm, $a_v = 0.73$ fm, and $a_w = 1.75$ fm. Analyzing the total cross-sections of reactions, which were identified with absorption cross-sections, all parameters of the optical potential were fixed and only the parameter a_w was varied. The results of calculations together with the measured values of σ_R are shown in Fig. 11.

The calculated values of σ_R agree with those measured for the interval $a_w = (1.65 \div 1.85)$ fm in the case of ^{58}Ni and $a_w = (1.94 \div 2.2)$ fm in the case of ^{64}Ni.

In view of the ambiguity of parameters of the optical potential, the equality sign should not be put between the obtained values of a_w and the thickness of the diffusive layer of a nucleus. One should consider this

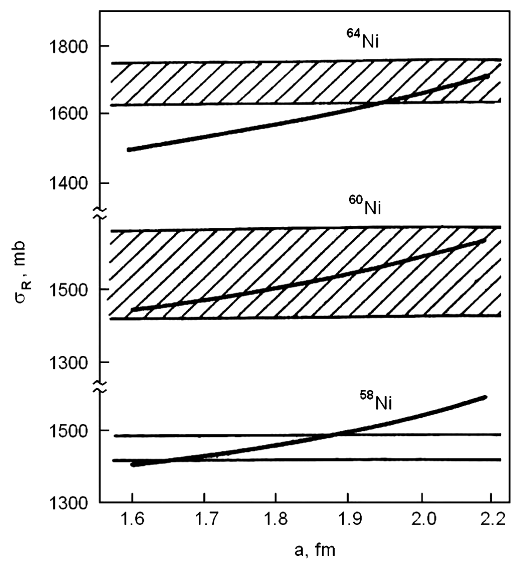

Fig. 11. Dependence of the total cross sections of reactions on isotopes of nickel for deuterons with an energy of 13.6 MeV. Shaded area – experimental values of σ_R with regard for the measurement errors

relationship as the qualitative indication of a possibility for the nucleus diffuseness to grow with increase in the relative neutron excess.

1. J.R. Oppenheimer, Phys. Rev. **47**, 845 (1935).
2. S.M. Dancoff, Phys. Rev. **72**, 1017 (1947).
3. L.D. Landau and E.M. Lifshits, Zh. Eksp. Teor. Fiz. **18**, 750 (1948).
4. C.J. Mullin and E. Guth, Phys. Rev. **82**, 141 (1951).
5. L.N. Rozentsveig and A.G. Sitenko, Zh. Eksp. Teor. Fiz. **30**, 427 (1956).
6. Y.M. Galicky, L.D. Landau, and A.B. Migdal, Physica **22**, 1168 (1956).
7. R. Gold and C. Wong, Phys. Rev. **132**, 2586 (1963).
8. A.I. Akhiezer and A.G. Sitenko, Uchen. Zap. Khar'k. Univ. **64**, 9 (1965).
9. E.L. Feinberg, Zh. Eksp. Teor. Fiz. **29**, 115 (1955).
10. R.J. Glauber, Phys. Rev. **99**, 1515 (1955).
11. H.E. Gove, Phys. Rev. **99**, 1353 (1955).
12. J.R. Rees and M.B. Sampson, Phys. Rev. **108**, 1289 (1957).
13. Yu.V. Gofman and O.F. Nemets, Zh. Eksp. Teor. Fiz. **39**, 1489 (1960).
14. Yu.V. Gofman and O.F. Nemets, Zh. Eksp. Teor. Fiz. **40**, 477 (1961).
15. O.F. Nemets, Ukr. Fiz. Zh. **8**, 505 (1983).
16. O.F. Nemets, M.V. Sokolov, and B.G. Struzhko, Congr. Int. Phys. Nucl. **2**, 961 (1964).

17. O.F. Nemets and R.G. Ofengenden, Visn. AN URSR **12**, 81 (1974).
18. O.F. Nemets, M.V. Sokolov, and B.G. Struzhko, Yad. Fiz. **1**, 1014 (1965).
19. O.F. Nemets, M.V. Sokolov, and B.G. Struzhko, Yad. Fiz. **4**, 521 (1966).
20. O.F. Nemets, V.M. Pugach, M.V. Sokolov, and B.G. Struzhko, Izv. Akad. Nauk SSSR. Ser. Fiz. **32**, 261 (1968).
21. O.F. Nemets, V.M. Pugach, M.V. Sokolov, and B.G. Struzhko, Reports of Intern. Sympos. on Nuclear Structure (JINR, Dubna, 1968), p. 123.
22. O.F. Nemets, V.M. Pugach, M.V. Sokolov, and B.G. Struzhko, Izv. Akad. Nauk SSSR. Ser. Fiz. **34**, 1714 (1970).
23. O.F. Nemets, V.M. Pugach, M.V. Sokolov, and B.G. Struzhko, Ukr. Fiz. Zh. **16**, 401 (1971).
24. S.T. Butler, Proc. Roy. Soc. A **208**, 559 (1951).
25. A.G. Sitenko and V.K. Tartakovsky, Ukr. Fiz. Zh. **4**, 708 (1959).
26. A.G. Sitenko and V.K. Tartakovsky, Ukr. Fiz. Zh. **6**, 12 (1961).
27. E.B. Levshin, Izv. Akad. Nauk SSSR. Ser. Fiz. **30**, 367 (1966).
28. Yu.A. Berezhnoi and E.V. Inopin, Yad. Fiz. **6**, 1197 (1967).
29. C.L. Fink, B.L. Cohen, J.C. van der Weerd, and R.J. Petty, Phys. Rev. **185**, 1568 (1969).
30. L. Jarczuk, J. Lang, and R. Müller, Phys. Lett. B **39**, 191 (1972).
31. L. Jarczuk, J. Lang, and R. Müller, Phys. Rev. C **8**, 68 (1972).
32. J. Lang, L. Jarczuk, and R. Müller, Nucl. Phys. A **204**, 97 (1973).
33. V.I. Grantsev, I.P. Dryapachenko, V.A. Kornilov, V.V. Metnev, O.F. Nemets, and M.V. Sokolov, Izv. Akad. Nauk SSSR. Ser. Fiz. **35**, 1747 (1971).
34. M.V. Evlanov, O.F. Nemets, M.V. Sokolov, and B.G. Struzhko, Izv. Akad. Nauk SSSR. Ser. Fiz. **37**, 1527 (1973).
35. V.I. Grantsev, I.P. Dryapachenko, V.A. Kornilov, O.F. Nemets, V.M. Pugach, B.A. Rudenko, M.V. Sokolov, and B.G. Struzhko, Izv. Akad. Nauk SSSR. Ser. Fiz. **41**, 156 (1977).
36. V.I. Grantsev, I.P. Dryapachenko, M.V. Evlanov, V.A. Kornilov, O.F. Nemets, V.M. Pugach, and B.G. Struzhko, Ukr. Fiz. Zh. **22**, 238 (1977).
37. V.I. Grantsev, I.P. Dryapachenko, M.V. Evlanov, V.A. Kornilov, O.F. Nemets, V.M. Pugach, M.V. Sokolov, and B.G. Struzhko, Ukr. Fiz. Zh. **22**, 243 (1977).
38. V.A. Zhmailo, Yad. Fiz. **12**, 239 (1970).
39. F. Becchetti and G. Greanleas, Phys. Rev. **182**, 1190 (1969).
40. G. Baur and D. Trautmann, Nucl. Phys. A **199**, 218 (1973).
41. A. Sommerfeld, *Atombau und Spektrallinien* (Vieweg, Braunschweig, 1931).
42. W. Hauser, H. Feshbach, Phys Rev. **87**, 366 (1952).
43. O.F. Nemets, L.I. Slyusarenko, and V.V. Tokarevsky, Elem. Chast. At. Yad. **6**, No. 4, 827 (1975).
44. O.P. Bilaniuk, V.S. Bulkin, L.V. Dubar, O.F. Nemets, L.I. Slyusarenko, and V.V. Tokarevsky, J. Phys. G **7**, 1699 (1981).
45. O.F. Nemets, L.S. Sokolov, V.V. Tokarevsky, and I.P. Chernov, Yad. Fiz. **4**, 293 (1966).

NEMETS OLEG FEDEROVYCH (13.02.1922–29.05.2002)

Oleg Federovych Nemets – physicist, Academician of National Academy of Sciences of Ukraine (elected in 1978), Professor (1963), Honored Scientist of Ukraine. Born in Kiev; he was the student of the Radio-Engineering Faculty of Kiev Polytechnic Institute in 1940–1947. During wartime, O.F. Nemets worked on a defense plant evacuated to Ural. From 1949 to 1970, he was an engineer, postgraduate, scientific associate, senior scientist, and Deputy Director of the Institute of Physics of Academy of Sciences of Ukrainian SSR. From 1965 to 2000 – head of the Department of Nuclear Reactions established at the Institute of Physics (in 1970, the department became the part of the Institute for Nuclear Research). From 1974 to 1983 – Director of the Institute for Nuclear Research Institute; from 2000 to 2002 – leading scientist of this institute.

O.F. Nemets is a founder of the Ukrainian scientific school on nuclear reactions. The scientist's activity covers many fundamental and applied directions of nuclear physics, nuclear power engineering, and environment protection. His researches of nuclear reaction mechanisms and the distribution of nuclear matter density, pioneer experiments on multiparticle reactions and polarization phenomena are widely known. In the international scientific literature, the isotopic dependence of deuteron break-up cross sections in the field of nuclei with different masses, which was revealed by the scientist, has been named later on as the "Nemets effect". For the first time under the leadership of O.F. Nemets, the g-factors of excited states of some nuclei were measured using the accelerator beam, and the influence of external Coulomb fields on the parameters of short-lived resonances produced in multiparticle reactions was ascertained.

O.F. Nemets is the author and co-author of many inventions and more than 300 scientific works, three monographs, two textbooks, and a handbook on nuclear physics. For his research and pedagogical activity, O. Nemets was awarded with two "Sign-of-Honor" orders, the Ukrainian "For Services" order of the third degree, Sinel'nikov's Prize of Academy of Sciences of UkrSSR, and Ukrainian State Prize in Science and Engineering.